

Utilization of CO₂ cured CSW-MSWIBA cold bonded aggregate into lightweight concrete products for masonry units

Yohannes L. Yaphary,^a Jian-Xin Lu,^a Bin Zhao,^b Hiu Wun Cheng,^a Peiliang Shen,^a Dongxing Xuan,^a and Chi Sun Poon^{*a}

^aDepartment of Civil and Environmental Engineering, The Hong Kong Polytechnic University,
Hung Hom, Kowloon, Hong Kong

^bChina Everbright Green Technology Innovation Research Institute, Hong Kong

*Correspondence should be addressed to C.S. Poon (email address: cecspoon@polyu.edu.hk)

1 **Highlights**

- 2 • CBA was made from the composite of CSW and MSWIBA.
- 3 • CBA can be utilized to produce lower-cost LWC masonry unit.
- 4 • LWC masonry unit is per ASTM C129 and C90.
- 5 • Hollow glass granulates can lower the thermal conductivity.

7 **Abstract**

8 Cold bonded aggregate (CBA) produced principally with concrete slurry waste (CSW) and
9 municipal solid waste incinerator bottom ash (MSWIBA) was used to produce lightweight
10 concretes products – precast masonry units (LWCMU). The properties of the concrete products
11 prepared with the 100% coarse CBA and different fractions of mixed fine CBA and hollow glass
12 granulates (HGG) were compared to produce CBA-LWCMU. The tested properties included dry
13 bulk density, compressive strength, absorption, drying shrinkage and thermal conductivity. It is
14 found that CBA-LWCMU can meet the requirement of non-loadbearing and loadbearing LWCMU
15 as per ASTM C129 and C90, respectively. The advantages of using CBA-LWCMU (i.e., as
16 compared to LWCMU made with sintered expanded clay aggregate) include lower cost and
17 thermal conductivity. The thermal conductivity of CBA-LWCMU can lead to better thermal
18 insulation and passive fire protection of masonry. Furthermore, it was discovered from
19 thermogravimetric analysis (TGA) and mercury intrusion porosimetry (MIP) tests that heated
20 HGG (i.e., as compared to CBA) has better thermal stability and its apparent density was increased
21 after being heated. These advantageous characteristics of HGG can lead to the improved fire
22 resistance of CBA-LWCMU exposed to the elevated temperature.

23 **Keywords**

24 Municipal solid waste incinerator bottom ash; Cold bonded aggregate; Lightweight concrete
25 masonry unit; Thermal conductivity



1. Introduction

Application of lightweight concrete masonry units (LWCMU) has obvious advantages in building construction, including low density, high thermal insulation and passive fire protection of the whole building [1, 2]. The relatively reduced density of LWCMU largely depends on the use of lightweight aggregate (LWA). In most cases, the LWA is used as coarse aggregate in LWC [3]. Natural LWA is scarce as it has particle density characteristics between 0.8 - 2.0 g/cm³, while most of the natural aggregates have particle densities of 2.4 - 2.8 g/cm³ [4]. There are several artificial commercially available LWAs, which are produced by high-temperature sintering processes. Amongst these, lightweight expanded clay aggregate (LECA) produced by the sintering processed clayey soil at about 1100 - 1300 °C [5] has been commonly used worldwide. Another alternative artificial LWA is hollow glass granulates (HGG), which are produced from sintering glass waste at a relatively lower temperature between 800 and 900 °C [6, 7]. However, the high energy consumption for producing the LWA involving a sintering process has motivated the exploration of producing alternative lightweight artificial aggregate [8].

In comparison with the sintering process, cold-bonding pelletization provides a low-energy process for manufacturing artificial cold bonded aggregates (CBA) [9]. Furthermore, the cold-bonding pelletization process also benefits from using industrial reactive by-products as the binder and industrial solid wastes as inclusion for granulation [10]. As reviewed by Tajra et al. [11], the physical properties of CBA are normally in the size of 4-20 mm with particle densities, loose bulk densities (LBD) and water absorptions of 880 - 2120 kg/m³, 510-1247 kg/m³ and 2.5-77%, respectively. The bulk crushing and individual particle strength are 0.2-15.7 MPa and 0.25-22.8 MPa, respectively [11]. Fly ash has been widely employed to produce CBA and fly ash geopolymer with NaOH activator results in relatively higher strength [12-14].

Recently, in order to effectively utilize incineration residues, municipal solid waste incinerator bottom ash (MSWIBA) (i.e., with particle size < 2.36 mm) and concrete slurry waste (CSW) at the fresh stage were used to produce MSWIBA-CSW CBA [15-17]. The production process is illustrated in Figure 1.

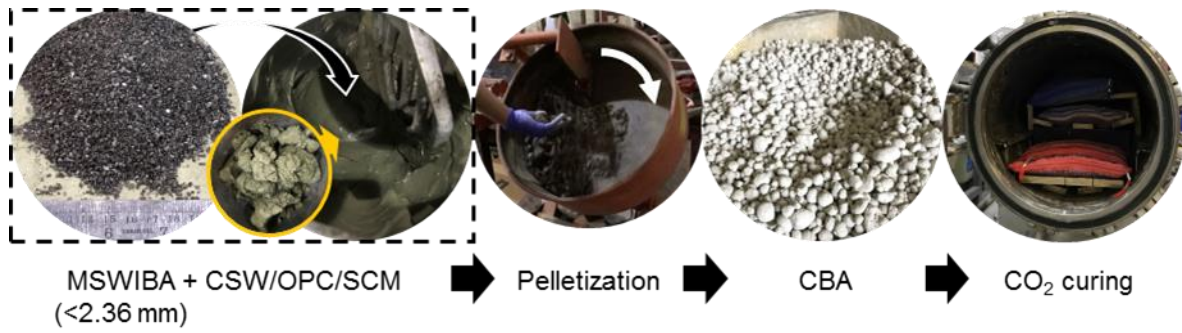


Figure 1. Production process of CBA by MSWIBA and CSW.

CSW is obtained from the aggregate reclaiming system of ready-mixed concrete batching plants, where over-ordered or rejected fresh concrete (i.e., including the concrete from cleaning the concrete mixer truck) is washed out to retrieve the aggregates [18, 19]. The production of CBA by using CSW and MSWIBA not only provides a recycling method to solve their disposal issue but also produces a new type of artificial aggregate. The range of LBD, water absorption and bulk crushing and individual particle strengths of MSWIBA-CSW CBA are $790\text{--}1025\text{ kg/m}^3$, 13-27%, 5.93 MPa and 0.3-8.0 MPa, respectively [15-17]. These properties varied with the addition of minor constitutes (i.e., ground-granulated blast-furnace slag (GGBS), silica fume or incineration sewage sludge ash (ISSA)) in the pelletization process and curing methods (i.e., moist, steam or CO_2 curing). However, in most cases, CBA still have a high LBD, which is more than two folds higher than the LECA (i.e., $305\text{--}560\text{ kg/m}^3$ depending on the particle size distribution) [20] and larger than 880 kg/m^3 . Therefore, these cannot be specified as lightweight aggregate based on ASTM C331 [21] and the competitiveness of CBA as compared to LECA as artificial aggregate for LWCMU production with the same specification remains a question. For instance, the OD densities of concretes produced with CBA lie between $1682\text{--}1981\text{ kg/m}^3$ [22-24]. The maximum OD density requirement for LWCMU (i.e., non-loadbearing and loadbearing) is 1680 kg/m^3 in ASTM C129 [25] and C90 [26].

The objective of the present study is to evaluate the feasibility of utilizing CBA (produced by MSWIBA and CSW) for producing lower-cost LWCMU with relatively lower thermal conductivity for better thermal insulation and passive fire protection.

2. Materials and experimental program

2.1. Materials

This mixture proportion of the produced CBA using MSWIBA and CSW was designed based on the findings from the previous studies that showed the use of small percentages of ordinary Portland cement (OPC) and ground-granulated blast-furnace slag (GGBS) as additional binders could significantly increase the strength of CBA [15]. Table 1 shows the oxide chemical compositions of binders (i.e., CSW, OPC and GGBS) used to produce the CBA. CSW was provided by a local ready-mixed concrete batching plant. The MSWIBA was obtained from an MSW incineration plant in Guangdong province, China. MSWIBA with the particle size of < 2.36 mm was used as an inclusion in the CBA. This MSWIBA has an absorption of 12.19% with saturated surface dry (SSD) and oven-dry (OD) particle density of 1.49 and 1.33 g/cm³, respectively. The mixture proportion used for producing the CBA is shown in Table 2. Wet CSW was used with water to a solid ratio of 1.18.

Table 1. Oxide chemical compositions of ordinary Portland cement (OPC), dried concrete slurry waste (CSW) and ground-granulated blast-furnace slag (GGBS) used to produce CBA.

Oxide component	OPC (%)	CSW (%)	GGBS (%)
SiO ₂	19.30	34.70	35.2
Al ₂ O ₃	5.35	11.40	17.40
Fe ₂ O ₃	3.25	4.09	0.48
CaO	64.80	42.00	34.30
MgO	0.91	2.02	8.13
K ₂ O	0.64	1.32	0.61
SO ₃	4.60	3.27	2.23
LOI	2.67	16.34	1.04

Table 2. Mixture proportion of cold bonded aggregate (CBA) by weight.

Material	Wet	OPC	GGBS	MSWIBA
	CSW			
Proportion	1	0.1	0.3	1.8

The CBA was made by following the procedures reported in our previous study [15]. First, the CSW (i.e., as delivered from the ready-mix concrete producer) was transformed into the paste by rapid mixing. Then, the GGBS and MSWIBA were mixed with CSW paste. Afterward, the pelletization of MSWIBA-CSW mixture was performed by using a rotating pelletizer. After curing in the laboratory condition (25 °C and 70 RH) for one day, the CBA was cured in a CO₂ chamber with a pressure of +0.1 bar for 8 hours as schematically shown in Figure 2. The CO₂ curing with a pressure of +0.1 bar resulted in an improved individual particle strength and lower water absorption [16]. After the process, about 3% CO₂ by weight of CBA can be captured. After curing, the CBA was then sieved to pass through 19 mm and retain on 4.75 mm. The remaining particle sizes of CBA were crushed into fine aggregate passing sieve opening of 4.75 mm.

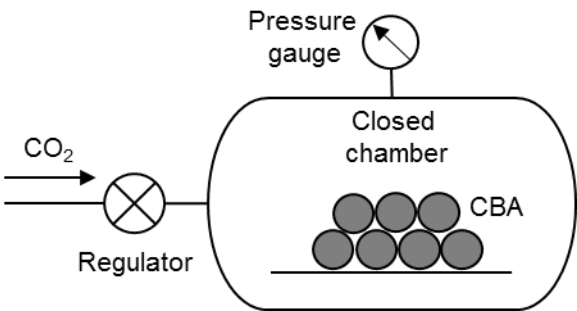


Figure 2. Schematic of CO₂ curing of CBA with a pressure of 0.1 bar for 8 hours.

To study the effects of fine and coarse CBA on LWCMU properties, the natural fine aggregate (NF) of crushed granite and LECA were used to make reference LWCMU. Additionally, HGG was used as inclusion into fine CBA to make LWCMU with 100% coarse CBA. Table 3 shows the SSD and OD particle densities, absorption, loose bulk density (LBD) and individual particle strength of fine and coarse aggregates. The particle densities and absorption of fine and coarse aggregates were measured as per ASTM C127 [27] and C128 [28], respectively. The LBD was determined as per ASTM C29 [29]. The compressive strengths of HGG, coarse CBA and

LECA were calculated by using Equation 1 [30]. Where σ is the compressive strength of the particle, P is the fracture force, and h is the distance between the loading point. The P was obtained by loading the particle with a speed of 0.6 mm/minute.

$$\sigma = \frac{2.8P}{\pi h^2} \quad (1)$$

The specific gravity and water absorption of CBA particles (i.e., the coarse particle size of 4.75 - 19 mm) were higher than those of LECA. The LBD of fine and coarse CBA is also higher than the LWA requirements in ASTM C331 [21]. According to ASTM C331 [21], the maximum LBD of LWA for fine and coarse aggregates is 1120 and 880 kg/m³, respectively. It should be noted that particle size distribution (PSD) affects the LBD. Therefore, similar aggregates with different PSD can result in a variety of LBD values. The LBD of coarse CBA in the present study is higher than those reported values (830-890 kg/m³) of the MSWIBA-CSW CBA containing GGBS and employing CO₂ curing in the existing studies [15, 16], which can be due to the different PSD of CBA used for the LBD measurement. The averaged (i.e., from the tests of 10 particles) crushing strength of individual CBA particle was 2.31 MPa, which was higher than 1.84 MPa of LECA.

Table 3. Saturated surface dry (SSD) and oven-dry (OD) specific gravities, water absorption, individual particle strength and dry loose bulk density (LBD) of aggregates. NF and HGG are fine natural aggregate and hollow glass granulates, respectively. The natural fine (NF) was obtained from crushing the natural granite into the fine aggregate of less than 4.75 mm.

Type of aggregate		SSD/OD specific gravity (g/cm ³)	water absorption at 24 hours (%)	Dry-LBD (kg/m ³)		Individual particle strength (MPa)
				Current study	ASTM C331 [21]	
Fine	NF	2.30/2.21	3.90	1781		-
	CBA < 4.75 mm	2.07/1.74	18.96	1185	≤ 1120	-
	CBA < 2.36 mm	2.08/1.74	19.51	1162		-
	HGG 2.36 – 4.75 mm	0.72/0.63	18.93	417		2.01
Coarse	LECA > 4.75 mm	0.79/0.70	12.70	475	≤ 880	1.84
	CBA > 4.75 mm	2.05/1.77	15.95	1000		2.31

2.2. Mix design of concrete

Based on the information of aggregate specific gravity, the concrete mixes with different aggregate proportions were designed by the volume method to reach the OD density lower or close to 1680 kg/m³. Two combinations of CBA < 2.36 mm and HGG with relatively low and high HGG portion (i.e., 30% and 80% by volume (b.v.) of HGG/CBA fine aggregate) were included to study the effect of HGG inclusion on the properties of CBA-LWCMU. The LBD of HGG/CBA-30/70 and 80/20 fine aggregates are 1042 and 772 kg/m³, respectively. The LBD of HGG/CBA fine aggregate is lower than that of fine CBA and can lead to the fine LWA as per ASTM C331 [21]. All the gradations of fine and coarse aggregates used in concretes are per ASTM C330 [31] with the nominal maximum size of 14 mm. The particle gradations and appearances of aggregates are shown in Figures 3 and 4, respectively.

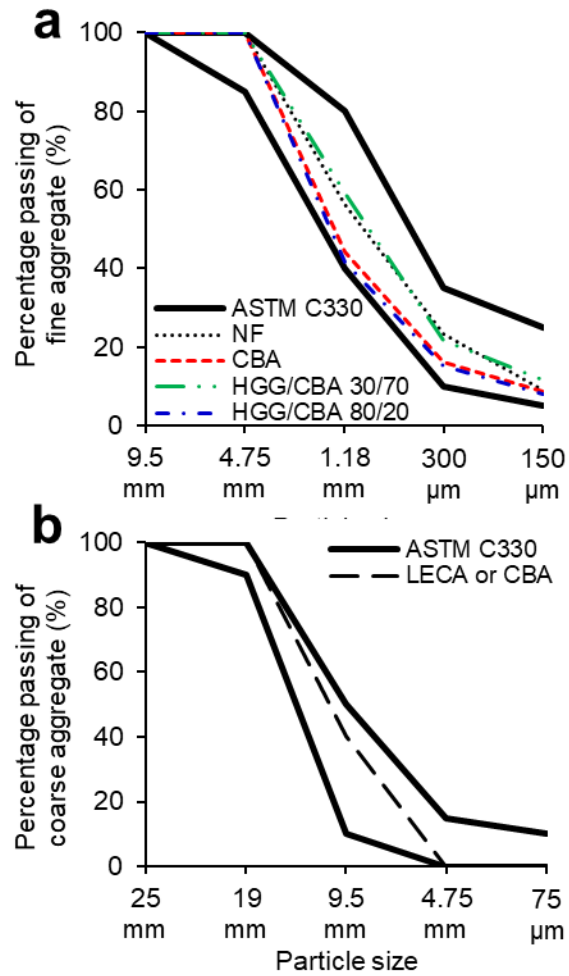


Figure 3. Particle gradations of (a) fine and (b) coarse aggregates.

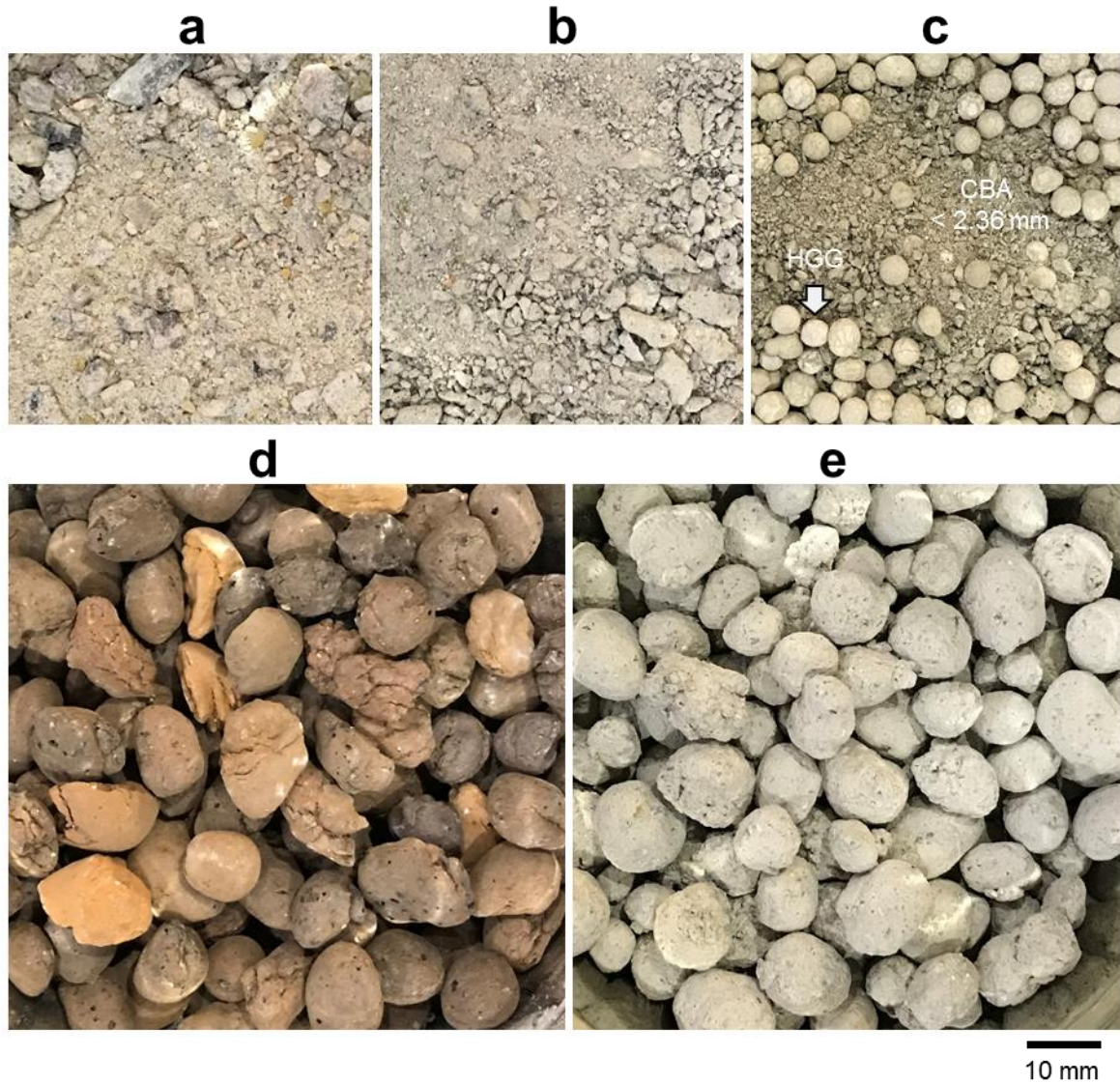


Figure 4. Fine aggregate of (a) NF, (b) CBA (i.e., < 4.75 mm) and (c) HGG/CBA mix. Coarse aggregate of (d) LECA and (e) CBA.

Table 4 shows the mixture proportion of concretes to study the effect of different aggregates on the concrete properties for the production of CBA-LWCMU. The nomenclature of concrete mixtures is in the form of FA(CBA content)-CA(CBA content), which indicates the CBA content for fine and coarse aggregates. FA0-CA0 indicates the reference concrete mixture that uses natural fine aggregate and LECA for coarse aggregate. FA100 denotes 100% fine CBA content as fine aggregate, and FA100-CA100 means the 100% content of fine and coarse CBA. The FA70 in FA70-CA100 indicates the combination of 70% of CBA < 2.36 mm and 30% of HGG b.v. for fine

aggregate (i.e., HGG/CBA-30/70 fine aggregate). Similarly, the FA20 in FA20-CA100 shows the combination of 20% of CBA < 2.36 mm and 80% of HGG b.v. for fine aggregate (i.e., HGG/CBA-80/20 fine aggregate).

Table 4. Mixture proportion of concrete per m³ by volume (b.v.)

Material	FA0-CA0	FA100-CA0	FA100-CA100	FA70-CA100	FA20-CA100
	b.v. (m ³)/b.w. (kg/m ³)				
Water	0.20/203	0.20/203	0.20/203	0.20/203	0.20/203
OPC	0.14/451	0.14/451	0.14/451	0.14/451	0.14/451
NF	0.26/599	-	-	-	-
CBA < 4.75 mm	-	0.26/539	0.26/539	-	-
CBA < 2.36 mm	-	-	-	0.18/377	0.05/108
HGG 2.36 – 4.75 mm	-	-	-	0.08/56	0.21/150
LECA > 4.75 mm	0.40/311	0.40/311	-	-	-
CBA > 4.75 mm	-	-	0.40/805	0.40/805	0.40/805

All concrete specimens were steam cured at 70°C for 24 hours to obtain the compressive strength of reference concrete higher than 13.8 MPa (i.e., the compressive strength requirement for loadbearing LWCMU according to ASTM C90 [26]). Previous studies showed that the optimum performance of concrete could be obtained by steam curing between 65 - 85 °C [32] and the common practice is to steam LWCMU for 24 hours [33]. After the steam curing, the specimen was placed in the ambient environment for additional 48 hours before testing in accordance with ASTM C140 [34]. The detailed procedures on different tests performed are described as follows.

2.3. Testing methods

2.3.1. Macroscale properties at ambient temperature

The tests on macroscale properties of concretes included oven-dry density, compressive strength, absorption (i.e., these tests were performed as per ASTM C140 [34]) and drying shrinkage. All the

specimen size was 50 x 50 x 50 mm³ (i.e., the minimum cross-sectional dimension of a rectangular section is larger than three times the aggregates' nominal maximum size as per ASTM C 192 [35]), unless otherwise mentioned. The concrete specimen (i.e., 75 x 75 x 285 mm³) and apparatus for drying shrinkage test were per ASTM C157 [36]. The drying shrinkage was determined based on the length difference between SSD and OD (i.e., with 50°C temperature up to constant mass and length) specimen as per ASTM C426 [37]. The additional test included thermal conductivity to investigate the thermal insulating property and passive fire protection. The thermal conductivity of LWC was tested by using the hot disk principle (Hot Disk, Hot Disk M1, SE) with a measurement range from 0.03 to 40 W/mK [38]. Following the 48 hours of conditioning in the ambient environment, the specimens were dried in an oven at 105 °C. Then, the specimens were cooled down in the ambient environment before thermal conductivity testing.

2.3.2. Heat transfer due to flame exposure

The heat transferability of concrete was examined by exposing the concrete specimen to the flame. The flame comes from a propane-butane gas torch (i.e., the temperature range is between 1093 to 1232 °C [39]) placed in front of a concrete block specimen (i.e., with a size of 200 x 100 x 60 mm) as schematically shown in Figure 5. The temperature evolution at the back of the specimen was measured by a thermocouple connected to a data logger. This setup has been adopted in the previous study [40] and can provide a comparison of the fire rating of LWCMU with LECA and CBA. The test was performed for 90 minutes (1.5 hours). This period is longer than the requirement of fire-resistance rating (i.e., between 3/4 to 1 hour) for concrete consisting of expanded clay with a thickness of 60 mm according to ACI 216 (i.e., code requirements for determining the fire resistance of concrete and masonry construction assemblies).

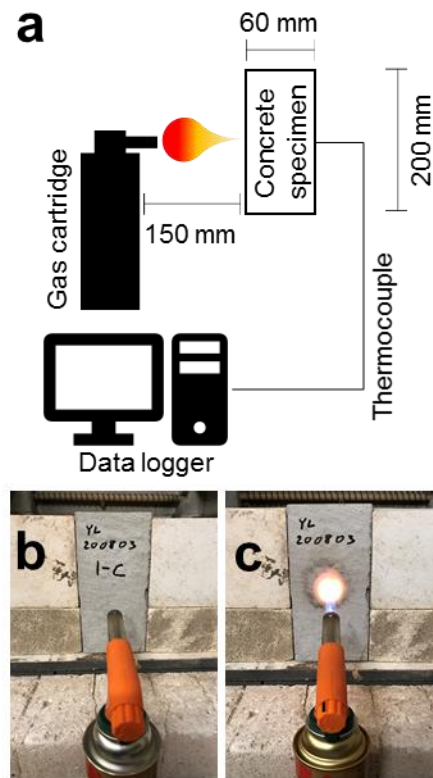


Figure 5. (a) Schematic of the setup for the flame exposure test. The flame comes from a propane-butane gas torch, and a concrete block specimen has a size of 200 x 100 x 60 mm. A typical snapshot showing the setup of the specimen and torch (a) before and (c) during flame exposure.

2.3.3. Elevated temperature characteristic of CBA and HGG

To find the insights by which the HGG influences the thermal conductivity (i.e., leading to improved thermal insulation and passive fire protection of CBA-LWCMU), TGA and MIP test were performed on both CBA and HGG to examine the comparison between them. TGA (Thermo plus EVO2 TG 8121 from Rigaku, Japan) was used to obtain the information upon the thermal stability of CBA and HGG under the exposure of elevated temperature. The TGA was performed by increasing the temperature up to 1000 °C at the rate of 10 °C/minute in the argon atmosphere. The MIP (Poresizer 9320 manufactured by Micromeritics, USA) was employed to probe the microstructures of CBA and HGG before and after the exposure to an 800 °C elevated temperature for 4 hours.

3. Results and discussion

3.1. Effects of HGG on the properties of LWCMU with 100% coarse CBA: CBA-LWCMU

Figure 6 shows the effect of partially or fully using CBA on the OD density, water absorption and compressive strength of concretes as compared to the requirement for non-loadbearing and loadbearing LWCMU in ASTM C129 [25] and C90 [26], respectively. The reference concrete prepared with NF and LECA (FA0-CA0) meets the requirement of LWCMU. It should have the OD density lower than 1680 kg/m^3 and maximum absorption of 18% for loadbearing LWCMU. The minimum compressive strength for non-loadbearing and loadbearing LWCMU is 4.14 and 13.8 MPa, respectively. The use of 100% CBA as fine and coarse aggregates (i.e., FA100-CA100) increased the OD density, absorption and compressive strength of concrete. These increments are consistent with the higher OD specific gravity, absorption and individual particle strength of CBA than those of LECA. It is implied that the characteristics of coarse aggregate play the dominant effects in defining the concrete properties. The dominant effects from coarse aggregate can be assigned to a higher volumetric portion of coarse aggregate. Although the strength and absorption of FA100-CA100 concrete meet the requirement for LWCMU, the increased OD density of FA100-CA100 is higher than the LWCMU limit. As expected, the replacement of CBA fine aggregate with a small portion of HGG decreases the OD density (i.e., due to lower OD specific gravity of HGG than that of CBA), as can be observed from FA70-CA100 concrete. Other effects of HGG that can be seen from this concrete are increasing absorption and lowering compressive strength. These effects can be attributed to the higher absorption and lower individual particle strength of HGG than those of CBA. Nevertheless, the OD density, absorption, compressive strength and drying shrinkage of FA70-CA100 meet the requirement for LWCMU in ASTM C129 [25] and C90 [26]. The concrete prepared with 100% coarse CBA and a high portion of HGG (i.e., FA20-CA100) met the OD density and compressive strength requirements of LWCMU, but its water absorption was higher than that specified for LWCMU.

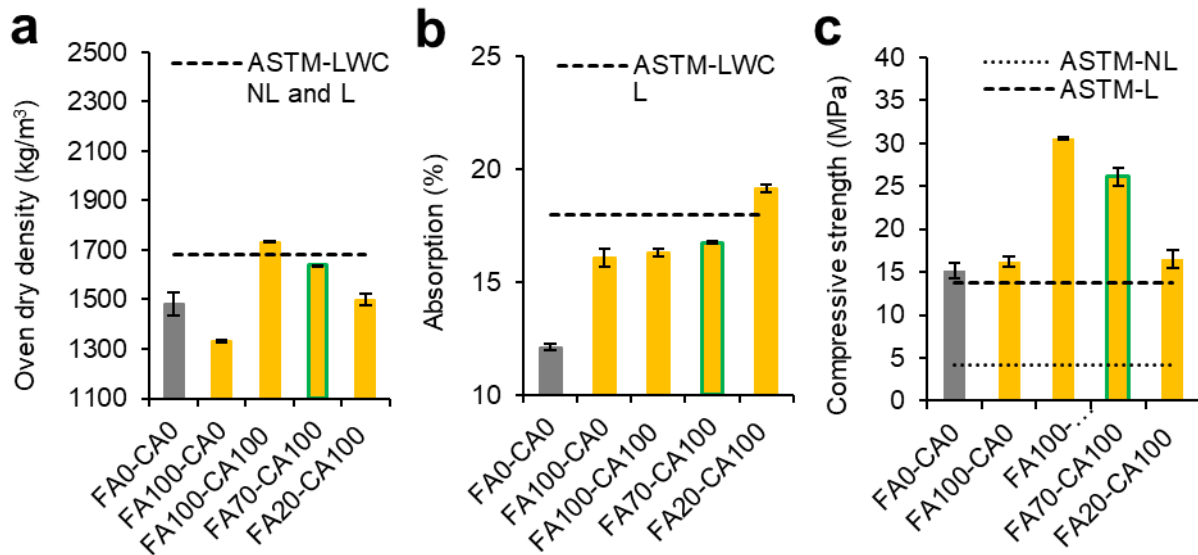


Figure 6. Effect of different aggregate types on the properties of concrete to comply with the requirements of lightweight concrete masonry unit (LWCMU) in ASTM C129 [25] (*i.e.*, non-loadbearing) and C90 [26] (*i.e.*, loadbearing). L and NL are non-loadbearing and loadbearing, respectively.

Figure 7 shows the comparison between the drying shrinkage of FA0-CA0, FA100-CA100 and FA70-CA100. The change from NF and LECA into fine and coarse CBA increases the drying shrinkage as expected. This increased drying shrinkage of FA100-CA100 concrete can primarily be due to the cementitious characteristic of CBA. CSW in CBA is principally cementitious material [41] [42], which naturally shrinks in the drying environment [43] [44]. Nonetheless, the increased drying shrinkage of mix FA100-CA100 concrete is within the LWCMU requirement and can be reduced by the inclusion of HGG, as indicated by the drying shrinkage of FA70-CA100 concrete.

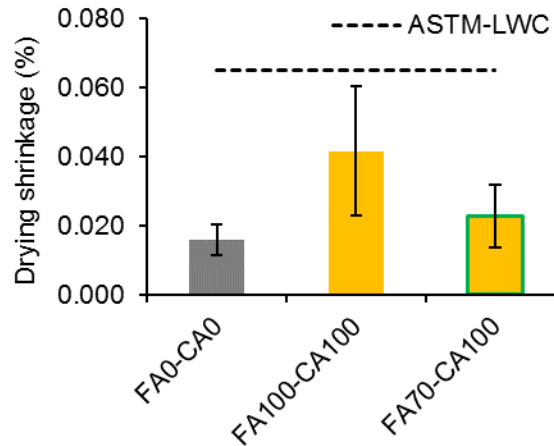


Figure 7. Drying shrinkage of FA0-CA0, FA100-CA-100 and FA70-CA100 concrete.

As per the effect of CBA and HGG fine aggregate on different concrete properties above, it is found that HGG can be used to decrease the OD density of concrete with 100% coarse CBA. Consequently, the LWCMU requirements can be met by the LWCMU with 100% coarse CBA. This can be observed from the properties of FA70-CA100 concrete. Another advantage of the HGG inclusion into the requirement of LWCMU property is reduced drying shrinkage. Table 5 summarizes the properties of FA70-CA100 concrete that meet the LWCMU requirements in ASTM C129 [25] and C90 [26]. It is therefore shown that LWCMU prepared with 100% coarse CBA (i.e., CBA-LWCMU) can be produced by adjusting the proportion of CBA and HGG for fine aggregate. It should be cautioned that the HGG inclusion should be minimized due to the adverse effects on absorption and compressive strength. In summary, the HGG decreases the OD density, drying shrinkage and compressive strength and increases absorption.

Table 5. Properties of FA70-CA100 concrete as compared to the LWCMU requirements in ASTM C129 [25] and C90 [26].

Properties	Density (kg/m ³)	Absorption (%)	Drying shrinkage (%)	Compressive strength (MPa)
FA70-CA100	1639	16.74	0.023	26.10
ASTM C129 [25]	≤ 1680	≤ 18	≤ 0.065	≥ 4.14
ASTM C90 [26]				≥ 13.8

3.2. Thermal conductivity of CBA-LWCMU

In a modern building, the desired functional advantages of using LWCMU for masonry are to provide thermal insulation for energy conservation and passive fire protection during the building's fire hazard. The thermal conductivity can largely indicate these functionalities. Figure 7 shows the thermal conductivities of FA0-CA0, FA100-CA100 and FA70-CA100 concrete. It can be seen that FA0-CA0 and FA100-CA100 concrete have similar thermal conductivity. This similarity can be attributed to the substitutions of both LECA and NF (i.e., in FA0-CA0) by CBA in FA100-CA100. The porosity of aggregate affects the thermal conductivity of concrete [45]. Changing LECA into less porous CBA increases the thermal conductivity. However, changing NF with more porous CBA can counteract such increment and result in similar thermal conductivity between FA0-CA0 and FA100-CA100 concretes. However, FA70-CA100 concrete has lower thermal conductivity. The lowering thermal conductivity from concrete specimen FA100-CA100 to FA70-CA100 exhibits the advantage from the HGG inclusion to reduce the thermal conductivity CBA-LWCMU. Moreover, the lower thermal conductivity of FA70-CA100 concrete indicates that CBA-LWCMU can provide better thermal insulation and passive fire protection for masonry than the one built from LWCMU made with NF and LECA.

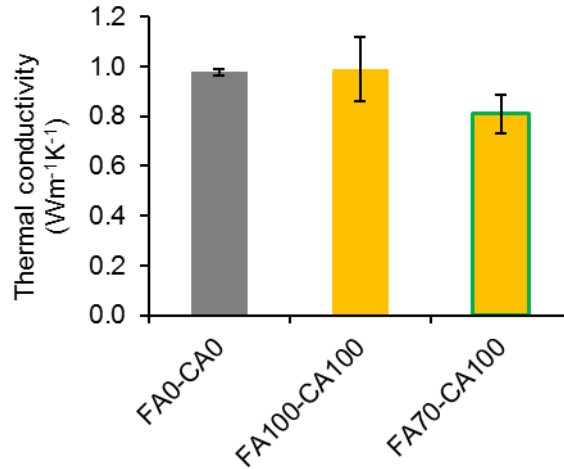


Figure 8. Thermal conductivity of the FA0-CA0, FA100-CA-100 and FA70-CA100 concrete.

Figure 9 shows the temperature evolution (i.e., measured from the non-exposed surface of the specimen) due to the heat transfer from the propane-butane gas flame into a 60 mm thick specimen. The comparison between the temperature evolution of the FA0-CA0 concrete and FA70-CA100 concrete indicates that CBA-LWCMU can provide better passive fire protection than the LWCMU made of NF and LECA. The lower temperature evolution on the non-exposed surface of FA70-CA100 concrete block specimen indicates that less heat has been transferred, and it agrees with the lower thermal conductivity of FA70-CA100 than that of FA0-CA0. As an example of the better passive fire protection of concrete with lower thermal conductivity is that it can prevent excessive heat and flame from spreading and provide longer escape time during the fire hazard. Figure 10 shows the concrete block specimens' condition before and after the flame exposure for 1.5 hours. The fired specimen was relatively still intact as compared to the initial condition. In the FA70-CA100 specimen case, the melting HGG was observed within the ring of the ignited area. The melted HGG provides an advantage to assist the visual assessment of the masonry part, which has been exposed to the elevated temperature and may need repair or replacement.

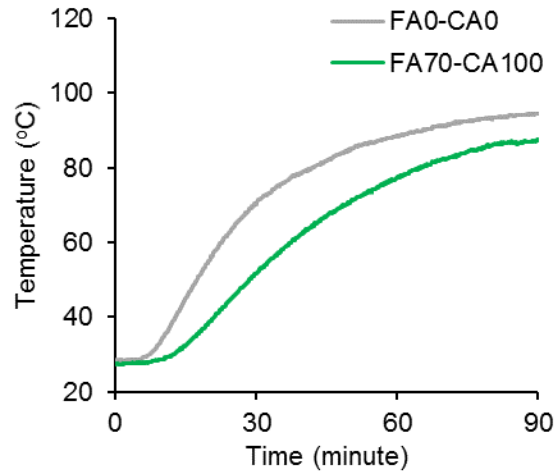


Figure 9. Temperature evolution measured (i.e., by a thermocouple) from the non-exposed surface of concrete block specimen (i.e., FA0-CA0 and FA70-CA100).

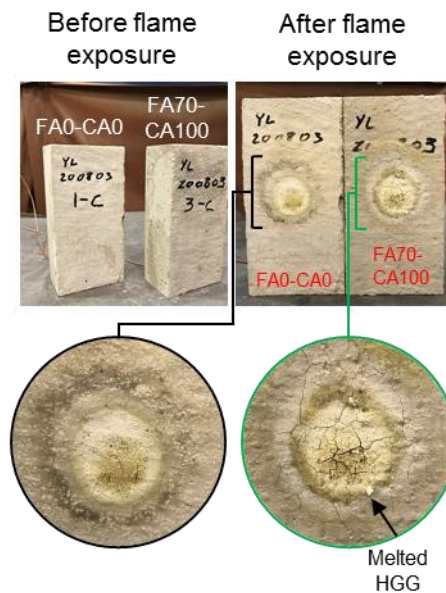


Figure 10. Specimen appearance of concrete block specimens (i.e., FA0-CA0 and FA70-CA100) before and after being the flame exposure.

3.3. Characteristic of CBA and HGG under elevated temperature exposure

In the previous section, it has been revealed that the presence of HGG in CBA-LWCMU can lower the thermal conductivity. To obtain an insight by which the HGG lowers the thermal conductivity of CBA-LWCMU, the elevated temperature (i.e., by heating to 800 °C for 4 hours) characteristics of CBA and HGG from MIP are compared and examined. Porosity has a significant role in defining

the thermal conductivity of porous materials like concrete [46]. The thermal conductivity of concrete decreases as the porosity increases [47]. Figure 11 shows that HGG has a higher porosity than CBA before and after heating. The higher porosity of HGG than CBA (i.e., before being heated) is consistent with the existing literature, which indicates HGG as more porous material than hydrated cement [7]. It should be cautioned when employing the MIP to compare the porosity of different materials. The porosity aspect of materials assessed by the MIP refers to the porosity that is accessible by the mercury intrusion. It is influenced by the pore characteristic and mercury's wetting characteristic for the solid interior part of porous material [48]. However, the agreement between the present study and existing literature on the relatively higher porosity of HGG indicates that the MIP can be employed to compare the HGG and CBA porosities. The higher porosity of HGG contributes to the lower thermal conductivity of CBA-LWCMU and continuously increases during flame exposure. As a consequence of lower thermal conductivity, the heat transfer capability of CBA-LWCMU is also reduced during flame exposure.

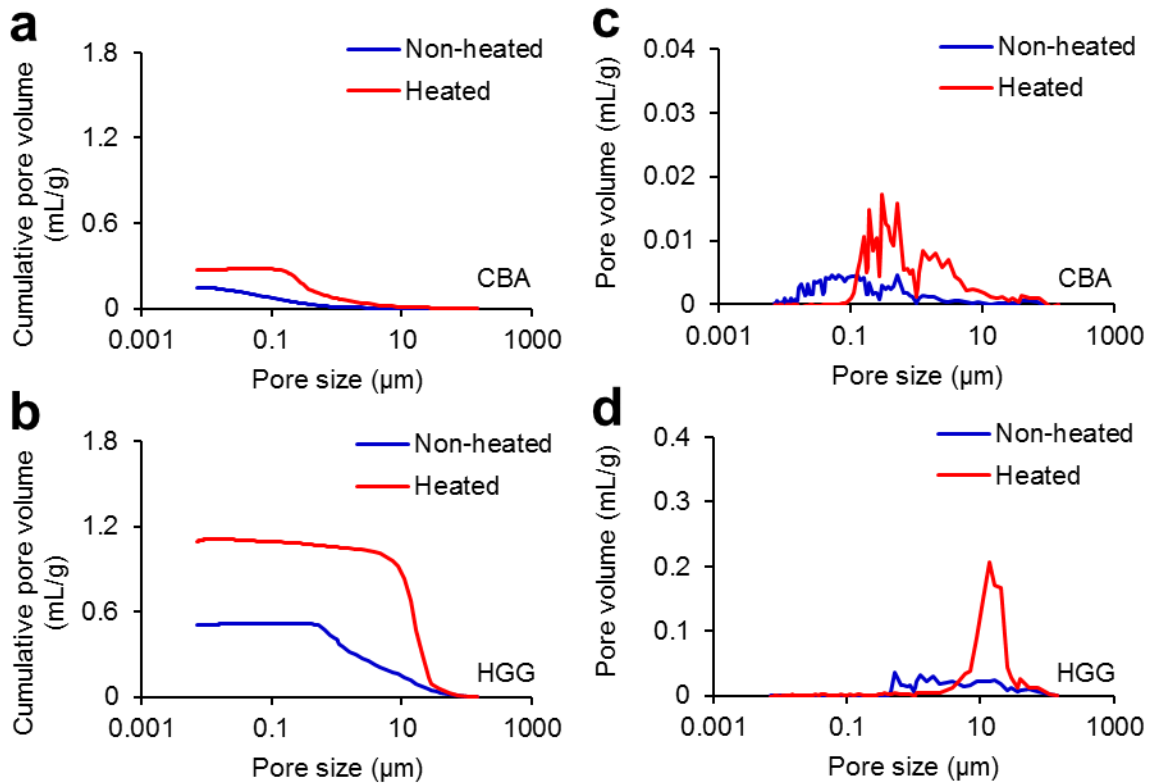


Figure 11. The pore structure of CBA and HGG as measured by mercury intrusion porosimetry (MIP). The cumulative pore volume of (a) CBA and (b) HGG. The distribution of pore volume of (a) CBA and (b) HGG.

Although the porosities of both CBA and HGG increases after heating, it is found that the compressive strength of individual HGG particle increases and that of CBA decreases, as shown in Figure 12a. CBA contains a substance similar to the product of hydrated cement, such as calcium-silicate-hydrate (C-S-H) and Ca(OH)_2 [49] [50]. These products come from the continuous hydration of partly hydrated cementitious and pozzolanic materials in CSW [51-54]. When being exposed to the elevated temperature, the hydration products decompose to lead to the increased porosity and lower mechanical properties [55]. Figure 12b shows the DTG curve of CBA that clearly indicated the decomposition of CaCO_3 [17]. This CaCO_3 product comes from the Ca(OH)_2 reaction with CO_2 in CSW during CO_2 curing [56]. In the case of HGG, the increased compressive strength of HGG after heating can be attributed to the denser skeletal structure of HGG. The apparent density of HGG was higher after being exposed to the elevated temperature as can be seen in Figure 12c. The increased strength of HGG after heating can increase the residual compressive strength of CBA-LWCMU (i.e., as shown in Figure 13), which hence can improve the resistance to fire performance.

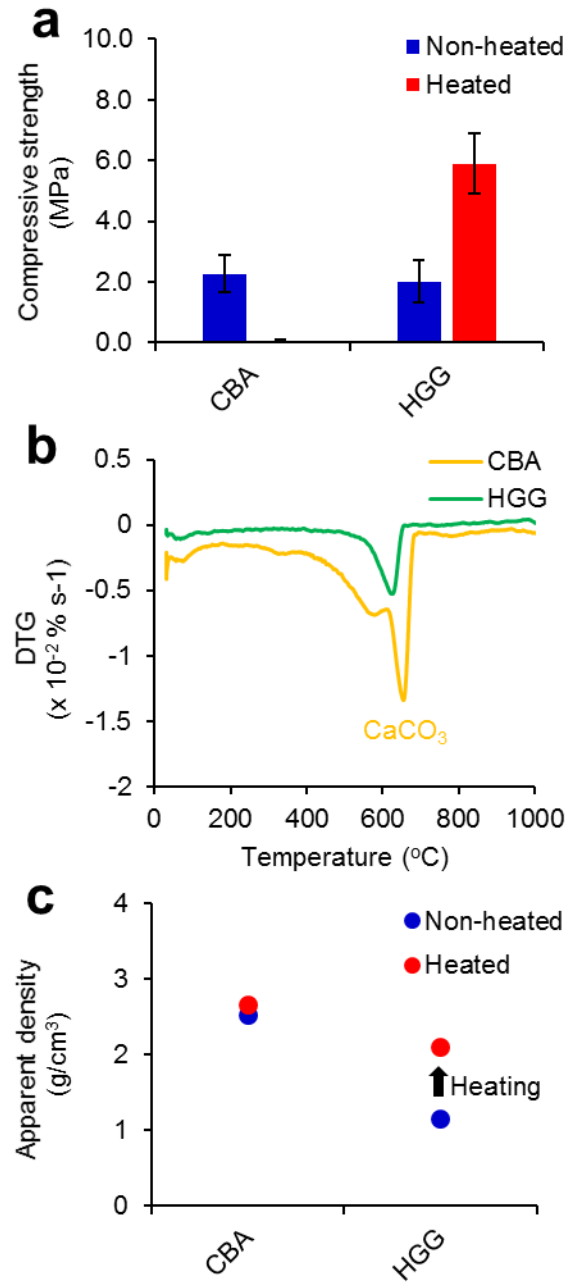


Figure 12. Compressive strength of individual CBA and HGG particles after being exposed to an elevated temperature of 800 °C for 4 hours.

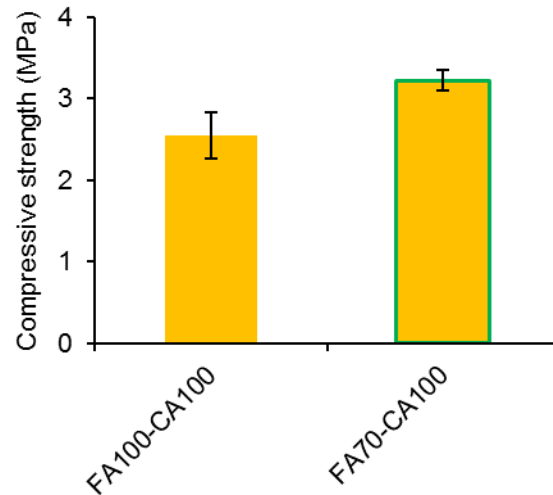


Figure 13. Compressive strength of FA100-CA100 and FA70-CA100 concretes after being exposed to an elevated temperature of 800 °C.

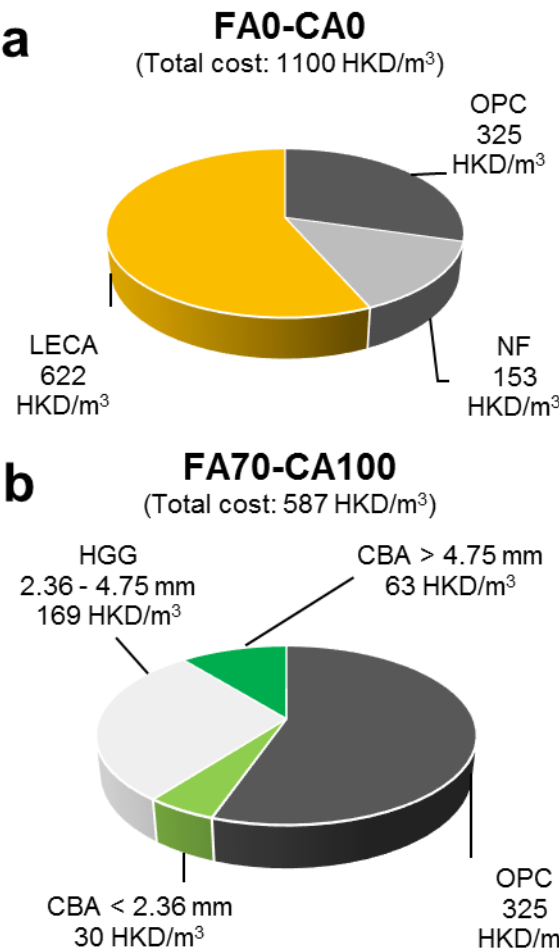
4. CBA-LWCMU cost

To evaluate the economic value from using CBA-LWCMU, the costs of FA0-CA0 and FA70-CA100 concrete were compared. Table 6 shows the ingredient unit cost (HKD/kg) and weight (kg/m³) of FA0-CA0 and FA70-CA100 concretes. All the ingredient unit costs were obtained from the local suppliers in Hong Kong. The unit cost of CBA was calculated by taking into account the unit cost of OPC and GGBS. The price of GGBS was 0.600 HKD/kg and CSW and MSWIBA were costless. Based on the unit cost and weight of concrete ingredients, the costs per m³ of FA0-CA0 and FA70-CA100 concretes were calculated. The result of this calculation is shown in Figure 14. It can be seen that FA70-CA100 concrete has a lower cost than FA0-CA0 concrete. The cost reduction from FA0-CA0 and FA70-CA100 concrete is due to CBA's lower material cost compared to NF and LECA. CBA's significantly lower material cost indicates that there is still space for production cost and a further feasibility study is worthwhile. Furthermore, CBA's material cost is useful information on cost estimation in the feasibility study for developing the low-cost production process of CBA.

415 Table 6. Unit cost and weight of ingredients of reference concrete and CBA-LWC 70/30.

Ingredients		Unit cost (HKD/kg)	Weight (kg/m ³)	
			Reference	CBA-LWC 70/30
Binder	Water	-	203	203
	OPC	0.720	451	451
Fine aggregate	NF	0.256	599	-
	CBA < 2.36 mm	0.079	-	377
	HGG 2.36 – 4.75 mm	3.000	-	56
Coarse aggregate	LECA > 4.75 mm	2.000	311	-
	CBA > 4.75 mm	0.079	-	805

416



417

418 Figure 14. Cost per m³ of (a) FA0-CA0 and (b) FA70-CA100.

5. Conclusion

In this study, the viability of utilizing the produced cold bonded aggregate (CBA) to prepare a lightweight concrete masonry unit (LWCMU) was evaluated. CBA was produced with a 95% by-product content of concrete slurry waste (CSW) and municipal solid waste incinerator bottom ash (MSWIBA). As compared to fine natural aggregate (NF) and lightweight expanded clay aggregate (LECA), the use of fine and coarse CBA increases the concrete density. To keep using 100% coarse CBA in LWCMU, the fine CBA was combined with the hollow glass granulate (HGG) as a fine aggregate to decrease the concrete density. It should be noted that the proportion of HGG should be minimized due to its adverse effect on the increased water absorption and decreased compressive strength of LWCMU. We find that LWCMU with 100% coarse CBA (i.e., called CBA-LWCMU) can be produced with fine aggregate composed of 70% fine CBA and 30% HGG proportion by volume. The properties of CBA-LWCMU meet the requirements of non-loadbearing and loadbearing LWCMU as per ASTM C129 [25] and C90 [26], respectively.

The advantages of CBA-LWCMU as compared to reference LWCMU (i.e., with NF and LECA coarse aggregate) are due to its higher compressive strength and lower thermal conductivity. This can provide better thermal insulation for energy conservation and passive fire protection during the fire hazard of the building. Furthermore, the presence of HGG is found to enhance the residual strength of CBA-LWCMU after being exposed to an elevated temperature of 800 °C for 4 hours. Such enhancement of the residual strength of CBA-LWCMU can be attributed to the increased compressive strength of individual HGG particles exposed to the elevated temperature. CBA-LWCMU also has a lower cost than reference LWCMU. The results from this study demonstrate the application viability of CBA to produce LWCMU, in which CBA is a sustainable product by using urban solid wastes of MSWIBA and CSW. This application can further aid to reduce the use of the natural resource (i.e., for being used as LWA) and keep energy conservation (i.e., due to lower energy consumption for cold-bonded pelletization) by recycling the CSW and MSWIBA into a less carbon footprint of the artificial aggregate of CBA.

Acknowledgements

The authors wish to thank the Innovation and Technology Support Programme (ITS-002-17FP), the Hong Kong Research Grants Council (PolyU 15223517) and the Hong Kong Polytechnic

University for funding support. Dr. Yohannes Lim Yaphary would express a special acknowledgment to Ms. Dorothy Chan and Mr. C.S. Liu for their sincere instrumental support.

References

- [1] P. Kanchanapiya, P. Methacanon, T. Tantisattayakul, Techno-economic analysis of light weight concrete block development from polyisocyanurate foam waste, *Resources, Conservation and Recycling* 138 (2018) 313-325.
- [2] S. Sahoo, A. Kumar, S.S. Prakash, Mechanical characterization of structural lightweight aggregate concrete made with sintered fly ash aggregates and synthetic fibres, *Cement and Concrete Composites* (2020) 103712.
- [3] M. Aslam, P. Shafigh, M.Z. Jumaat, M. Lachemi, Benefits of using blended waste coarse lightweight aggregates in structural lightweight aggregate concrete, *Journal of Cleaner Production* 119 (2016) 108-117.
- [4] C. Cheeseman, A. Makinde, S. Bethanis, Properties of lightweight aggregate produced by rapid sintering of incinerator bottom ash, *Resources, Conservation and Recycling* 43(2) (2005) 147-162.
- [5] A.M. Rashad, Lightweight expanded clay aggregate as a building material—An overview, *Construction and Building Materials* 170 (2018) 757-775.
- [6] P. Hrma, Effect of heating rate on glass foaming: Transition to bulk foam, *Journal of non-crystalline solids* 355(4-5) (2009) 257-263.
- [7] M. Limbachiya, M.S. Meddah, S. Fotiadou, Performance of granulated foam glass concrete, *Construction and building Materials* 28(1) (2012) 759-768.
- [8] S. İpek, O.A. Ayodele, K. Mermerdaş, Influence of artificial aggregate on mechanical properties, fracture parameters and bond strength of concretes, *Construction and Building Materials* 238 (2020) 117756.
- [9] F. Colangelo, F. Messina, R. Cioffi, Recycling of MSWI fly ash by means of cementitious double step cold bonding pelletization: Technological assessment for the production of lightweight artificial aggregates, *Journal of hazardous materials* 299 (2015) 181-191.
- [10] F. Colangelo, F. Messina, L. Di Palma, R. Cioffi, Recycling of non-metallic automotive shredder residues and coal fly-ash in cold-bonded aggregates for sustainable concrete, *Composites Part B: Engineering* 116 (2017) 46-52.
- [11] F. Tajra, M.A. Elrahman, D. Stephan, The production and properties of cold-bonded aggregate and its applications in concrete: A review, *Construction and Building Materials* 225 (2019) 29-43.
- [12] P. Gomathi, A. Sivakumar, Characterization on the strength properties of pelletized fly ash aggregate, *ARPN Journal of Engineering and Applied Sciences* 7(11) (2012) 1523-1532.
- [13] P. Gomathi, A. Sivakumar, D. Singh, A. Rajaraman, V. Sounthararajan, Crushing strength properties of furnace slag-fly ash blended lightweight aggregates, *ARPN Journal Engineering and Applied Sciences* 8(4) (2013) 246-251.
- [14] P. Gomathi, A. Sivakumar, Accelerated curing effects on the mechanical performance of cold bonded and sintered fly ash aggregate concrete, *Construction and building Materials* 77 (2015) 276-287.
- [15] P. Tang, D. Xuan, C.S. Poon, D.C. Tsang, Valorization of concrete slurry waste (CSW) and fine incineration bottom ash (IBA) into cold bonded lightweight aggregates (CBLAs):

- Feasibility and influence of binder types, *Journal of hazardous materials* 368 (2019) 689-697.
- [16] P. Tang, D. Xuan, H.W. Cheng, C.S. Poon, D.C. Tsang, Use of CO₂ curing to enhance the properties of cold bonded lightweight aggregates (CBLAs) produced with concrete slurry waste (CSW) and fine incineration bottom ash (IBA), *Journal of hazardous materials* 381 (2020) 120951.
- [17] P. Tang, D. Xuan, J. Li, H.W. Cheng, C.S. Poon, D.C. Tsang, Investigation of cold bonded lightweight aggregates produced with incineration sewage sludge ash (ISSA) and cementitious waste, *Journal of Cleaner Production* 251 (2020) 119709.
- [18] M.U. Hossain, D. Xuan, C.S. Poon, Sustainable management and utilisation of concrete slurry waste: A case study in Hong Kong, *Waste management* 61 (2017) 397-404.
- [19] D. Xuan, B. Zhan, C.S. Poon, W. Zheng, Innovative reuse of concrete slurry waste from ready-mixed concrete plants in construction products, *Journal of hazardous materials* 312 (2016) 65-72.
- [20] K.S. Al-Jabri, A. Hago, A. Al-Nuaimi, A. Al-Saidy, Concrete blocks for thermal insulation in hot climate, *Cement and Concrete Research* 35(8) (2005) 1472-1479.
- [21] ASTM C331 / C331M-17, Standard Specification for Lightweight Aggregates for Concrete Masonry Units, ASTM International, West Conshohocken, PA, 2017, www.astm.org.
- [22] N.U. Kockal, T. Ozturan, Durability of lightweight concretes with lightweight fly ash aggregates, *Construction and Building Materials* 25(3) (2011) 1430-1438.
- [23] R. Cioffi, F. Colangelo, F. Montagnaro, L. Santoro, Manufacture of artificial aggregate using MSWI bottom ash, *Waste management* 31(2) (2011) 281-288.
- [24] F. Colangelo, R. Cioffi, Use of cement kiln dust, blast furnace slag and marble sludge in the manufacture of sustainable artificial aggregates by means of cold bonding pelletization, *Materials* 6(8) (2013) 3139-3159.
- [25] ASTM C129-17, Standard Specification for Nonloadbearing Concrete Masonry Units, ASTM International, West Conshohocken, PA, 2017, www.astm.org.
- [26] ASTM C90-16a, Standard Specification for Loadbearing Concrete Masonry Units, ASTM International, West Conshohocken, PA, 2016, www.astm.org.
- [27] ASTM C127-15, Standard Test Method for Relative Density (Specific Gravity) and Absorption of Coarse Aggregate, ASTM International, West Conshohocken, PA, 2015, www.astm.org.
- [28] ASTM C128-15, Standard Test Method for Relative Density (Specific Gravity) and Absorption of Fine Aggregate, ASTM International, West Conshohocken, PA, 2015, www.astm.org.
- [29] ASTM C29 / C29M-17a, Standard Test Method for Bulk Density ("Unit Weight") and Voids in Aggregate, ASTM International, West Conshohocken, PA, 2017, www.astm.org.
- [30] Y. Li, D. Wu, J. Zhang, L. Chang, D. Wu, Z. Fang, Y. Shi, Measurement and statistics of single pellet mechanical strength of differently shaped catalysts, *Powder technology* 113(1-2) (2000) 176-184.
- [31] ASTM C330 / C330M-17a, Standard Specification for Lightweight Aggregates for Structural Concrete, ASTM International, West Conshohocken, PA, 2017, www.astm.org.
- [32] S. Türkel, V. Alabas, The effect of excessive steam curing on Portland composite cement concrete, *Cement and Concrete Research* 35(2) (2005) 405-411.
- [33] C. Shi, D. Wang, F. He, M. Liu, Weathering properties of CO₂-cured concrete blocks, *Resources, conservation and recycling* 65 (2012) 11-17.

- [34] ASTM C140 / C140M-20a, Standard Test Methods for Sampling and Testing Concrete Masonry Units and Related Units, ASTM International, West Conshohocken, PA, 2020, www.astm.org.
- [35] ASTM C192 / C192M-19, Standard Practice for Making and Curing Concrete Test Specimens in the Laboratory, ASTM International, West Conshohocken, PA, 2019, www.astm.org.
- [36] ASTM C157 / C157M-17, Standard Test Method for Length Change of Hardened Hydraulic-Cement Mortar and Concrete, ASTM International, West Conshohocken, PA, 2017, www.astm.org.
- [37] ASTM C426-16, Standard Test Method for Linear Drying Shrinkage of Concrete Masonry Units, ASTM International, West Conshohocken, PA, 2016, www.astm.org.
- [38] S. Yang, T.-C. Ling, H. Cui, C.S. Poon, Influence of particle size of glass aggregates on the high temperature properties of dry-mix concrete blocks, *Construction and Building Materials* 209 (2019) 522-531.
- [39] M. Porter, *Gas Burners for Forges, Furnaces, & Kilns*, Skipjack Press, Inc. 2004.
- [40] K. Mróz, M. Tekieli, I. Hager, Feasibility Study of Digital Image Correlation in Determining Strains in Concrete Exposed to Fire, *Materials* 13(11) (2020) 2516.
- [41] X. He, Z. Zheng, M. Ma, Y. Su, J. Yang, H. Tan, Y. Wang, B. Strnadel, New treatment technology: The use of wet-milling concrete slurry waste to substitute cement, *Journal of Cleaner Production* 242 (2020) 118347.
- [42] Y. Jiang, T.-C. Ling, M. Shi, Strength enhancement of artificial aggregate prepared with waste concrete powder and its impact on concrete properties, *Journal of Cleaner Production* 257 (2020) 120515.
- [43] F. Rajabipour, G. Sant, J. Weiss, Interactions between shrinkage reducing admixtures (SRA) and cement paste's pore solution, *Cement and Concrete Research* 38(5) (2008) 606-615.
- [44] Y.L. Yaphary, R.H. Lam, D. Lau, Reduction in cement content of normal strength concrete with used engine oil (UEO) as chemical admixture, *Construction and Building Materials* 261 (2020) 119967.
- [45] S. Real, J.A. Bogas, M.d.G. Gomes, B. Ferrer, Thermal conductivity of structural lightweight aggregate concrete, *Magazine of Concrete Research* 68(15) (2016) 798-808.
- [46] I. Asadi, P. Shafigh, Z.F.B.A. Hassan, N.B. Mahyuddin, Thermal conductivity of concrete—A review, *Journal of Building Engineering* 20 (2018) 81-93.
- [47] J. Chen, H. Wang, P. Xie, H. Najm, Analysis of thermal conductivity of porous concrete using laboratory measurements and microstructure models, *Construction and Building Materials* 218 (2019) 90-98.
- [48] R. Kumar, B. Bhattacharjee, Study on some factors affecting the results in the use of MIP method in concrete research, *Cement and Concrete Research* 33(3) (2003) 417-424.
- [49] Y.L. Yaphary, D. Lau, F. Sanchez, C.S. Poon, Effects of sodium/calcium cation exchange on the mechanical properties of calcium silicate hydrate (CSH), *Construction and Building Materials* 243 (2020) 118283.
- [50] J.W. Bullard, H.M. Jennings, R.A. Livingston, A. Nonat, G.W. Scherer, J.S. Schweitzer, K.L. Scrivener, J.J. Thomas, Mechanisms of cement hydration, *Cement and Concrete Research* 41(12) (2011) 1208-1223.

- 584 [51] D. Xuan, C.S. Poon, W. Zheng, Management and sustainable utilization of processing
585 wastes from ready-mixed concrete plants in construction: A review, *Resources,*
586 *Conservation and Recycling* 136 (2018) 238-247.
- 587 [52] H.A. Ali, D. Xuan, C.S. Poon, Assessment of long-term reactivity of initially lowly-reactive
588 solid wastes as supplementary cementitious materials (SCMs), *Construction and Building*
589 *Materials* 232 (2020) 117192.
- 590 [53] P. Suraneni, A. Hajibabae, S. Ramanathan, Y. Wang, J. Weiss, New insights from
591 reactivity testing of supplementary cementitious materials, *Cement and Concrete*
592 *Composites* 103 (2019) 331-338.
- 593 [54] S. Kang, Z. Lloyd, T. Kim, M.T. Ley, Predicting the compressive strength of fly ash
594 concrete with the Particle Model, *Cement and Concrete Research* 137 (2020) 106218.
- 595 [55] I. Janotka, T. Nürnbergerová, Effect of temperature on structural quality of the cement paste
596 and high-strength concrete with silica fume, *Nuclear Engineering and design* 235(17-19)
597 (2005) 2019-2032.
- 598 [56] D. Xuan, B. Zhan, C.S. Poon, W. Zheng, Carbon dioxide sequestration of concrete slurry
599 waste and its valorisation in construction products, *Construction and building materials*
600 113 (2016) 664-672.
- 601
- 602